



OPEN

On-chip immobilization of planarians for *in vivo* imaging

SUBJECT AREAS:

REGENERATION

LAB-ON-A-CHIP

IMAGING

MODEL INVERTEBRATES

Joseph P. Dexter^{1,2}, Mary B. Tammé³, Christine H. Lind³ & Eva-Maria S. Collins^{1,3,4}

¹Lewis-Sigler Institute for Integrative Genomics, Princeton University, Princeton, NJ 08544 USA, ²Department of Chemistry, Princeton University, Princeton, NJ 08544 USA, ³Department of Physics, University of California, San Diego, La Jolla, CA 92093 USA, ⁴Division of Biology, University of California, San Diego, La Jolla, CA 92093.

Received
8 July 2014

Accepted
14 August 2014

Published
17 September 2014

Correspondence and
requests for materials
should be addressed to
E.-M.S.C. (emscollins@
physics.ucsd.edu)

Planarians are an important model organism for regeneration and stem cell research. A complete understanding of stem cell and regeneration dynamics in these animals requires time-lapse imaging *in vivo*, which has been difficult to achieve due to a lack of tissue-specific markers and the strong negative phototaxis of planarians. We have developed the Planarian Immobilization Chip (PIC) for rapid, stable immobilization of planarians for *in vivo* imaging without injury or biochemical alteration. The chip is easy and inexpensive to fabricate, and worms can be mounted for and removed after imaging within minutes. We show that the PIC enables significantly higher-stability immobilization than can be achieved with standard techniques, allowing for imaging of planarians at sub-cellular resolution *in vivo* using brightfield and fluorescence microscopy. We validate the performance of the PIC by performing time-lapse imaging of planarian wound closure and sequential imaging over days of head regeneration. We further show that the device can be used to immobilize *Hydra*, another photophobic regenerative model organism. The simple fabrication, low cost, ease of use, and enhanced specimen stability of the PIC should enable its broad application to *in vivo* studies of stem cell and regeneration dynamics in planarians and *Hydra*.

Freshwater planarians are a popular model organism for studying stem cell biology and regeneration^{1–4} because of their large population of pluripotent adult stem cells, strong regenerative capabilities, and ease of breeding and manipulation. In addition, the development of molecular biology techniques for planarians, such as RNA interference (RNAi)⁵, immunohistochemistry^{4,6–7}, RNA sequencing^{8–10}, EST¹¹, and genome databases¹², has allowed researchers to undertake detailed studies of gene function during regeneration^{9,13–14}. One limitation to current planarian research, however, is a lack of effective techniques for live imaging. Planarians are negatively phototactic in the entire visible spectrum¹⁵, making immobilization of an animal for *in vivo* imaging at (sub-)cellular resolution a major challenge. Current methods for planarian immobilization include anesthetizing with chloretone (1,1,1-trichloro-2-methyl-2-propanol)¹⁶ or ethanol¹⁷, or embedding in low melting point agarose. There are major drawbacks to all existing immobilization techniques. Anesthetics have significant biological side effects, and mounting planarians in agarose is extremely low-throughput. Additionally, neither technique provides sufficient stability of immobilization for high-magnification imaging.

The use of microfluidic systems has emerged as a powerful approach to enable immobilization for high-resolution imaging, direct *in vivo* manipulation, and high-throughput screens of a variety of organisms including *Drosophila melanogaster* embryos and larvae^{18–22}, *Caenorhabditis elegans*^{21,23–31}, and zebrafish (*Danio rerio*) embryos and larvae^{32–35}. Immobilization of freshwater planarians, however, presents several unique challenges: Planarians are about an order of magnitude larger than *C. elegans*, have a squishy, readily deformed body, vary in size depending on the species, feeding state, last asexual reproduction event, and other factors³⁶, and are significantly more photophobic than *C. elegans* or *D. melanogaster* larvae. These characteristics make it infeasible to apply existing microfluidic immobilization techniques directly to planarians, which prompted us to develop an alternative method.

Here we describe the Planarian Immobilization Chip (PIC) for the imaging of live, physiologically active freshwater planarians (Fig. 1). We sought to develop a reliable device that is easy and inexpensive to fabricate without the use of specialized equipment and that would make live imaging accessible to the entire planarian community. By direct, quantitative comparison with conventional techniques, we show that the PIC significantly enhances imaging quality and duration. We then demonstrate that the stability achieved is sufficient to obtain high quality two-channel fluorescence imaging. Our device can immobilize planarians of different species and of various sizes for at least 5 hours without causing injury. Removing worms from the chip takes at most several minutes, and the PIC is therefore appropriate for medium-to-high throughput worm screens. We leveraged the

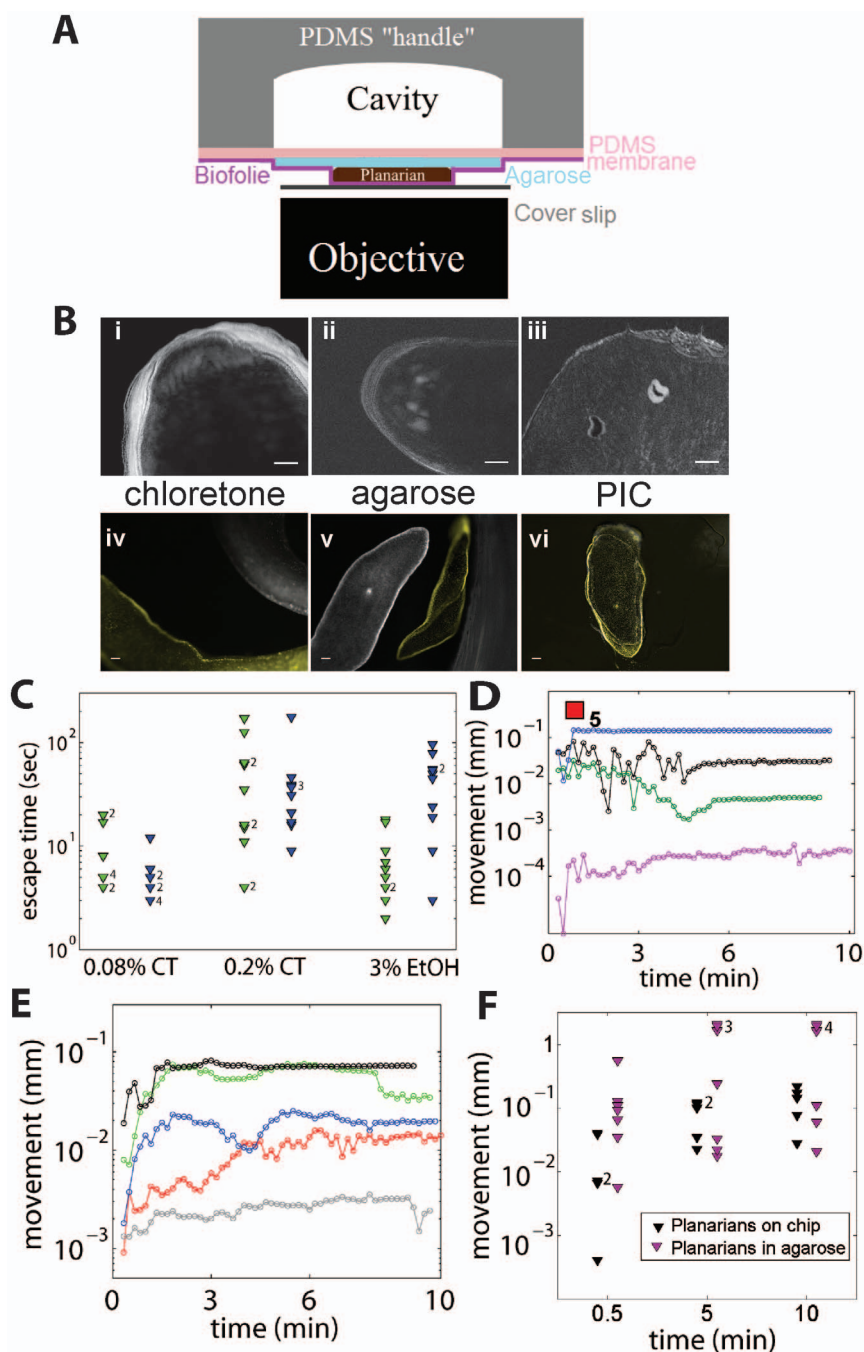


Figure 1 | Immobilization of live planarians. (A) Schematic of the PIC. (B) Qualitative comparison of the effectiveness of the PIC (iii, vi) to standard immobilization techniques such as the narcotic chlorotone (i, iv) and mounting in agarose (ii, v) with low-intensity white light and UV exposure. Scale bar: 100 μm . (C–F) Quantitative assessment of immobilization techniques. (C) The escape time is plotted for worms anesthetized following the three anesthesia protocols (0.08% chlorotone, 0.2% chlorotone, and 3% ethanol) and exposed to 560 nm (green triangles) or 350 nm (blue triangles) light. For all conditions $n = 10$; some data points were obtained more than once (indicated by superscripts). Planarians embedded in agarose or mounted on the PIC never left the field of view. (D, E) Tracking of the ocelli of planarians immobilized in agarose (D) and on the PIC (E). Only four out of nine planarians embedded in agarose could be tracked (the red square indicates the five failures). All samples (5) on the PIC could be tracked and showed minimal movement. (F) Movement of planarians exposed to UV light during on-chip and agarose immobilization. 10 minute movies were taken of worms stained with Hoechst 33342 and immobilized in agarose or on the PIC. Composite images were generated by superimposing the initial frame with frames at 30 seconds, 5 minutes, and 10 minutes, respectively (Fig. 1 (B) shows sample images). We found the position of the center of mass of the worm at the 4 time points using Image J and calculated the Euclidean distances that planarians on the chip (black triangles; $n = 5$) and planarians in agarose (purple triangles; $n = 7$) moved from their starting positions. Some data points were obtained more than once (indicated by superscripts).

enhanced stability and minimal invasiveness of the PIC to perform two planarian imaging experiments that would be unfeasible using standard immobilization techniques. The PIC's ease of use and negligible impact on worm health allows for removal and remounting of

specimens at will. As such, the PIC can be used for longitudinal observation of the same animal over long time scales. As a proof of principle, we imaged planarians over several days following decapitation and obtained an anatomical characterization of head regen-



eration. Additionally, we used the PIC as a platform for uninterrupted time-lapse microscopy of recently injured planarians over several hours, which yielded detailed dynamical information about wound closure.

Although the PIC was designed specifically for planarian immobilization, we also tested it on specimens of *Hydra vulgaris*, another photophobic regenerative model organism for which no effective immobilization and live imaging techniques exist. The chip can be directly applied to *Hydra* immobilization without any modifications and allows for dual-channel confocal microscopy of transgenic *Hydra* with excellent stability. The PIC thus has the potential to be a generic method for mounting small aquatic animals for live imaging at minimal cost. To facilitate broad adoption of the PIC, the Supplemental Material includes a detailed video protocol illustrating device fabrication and use (Movie S1).

Results

On-chip immobilization of live planarians. Planarian immobilization is accomplished by pressing a (poly)dimethylsiloxane (PDMS) membrane (attached to a solid PDMS base) over the body of the planarian to restrict movement (Fig. 1 (A)). PDMS membranes have previously been used in *C. elegans* immobilization devices^{24–25,37}, but our device has been customized for planarians through the incorporation of several non-PDMS components. To reduce specimen movement, liquid is removed, and the PDMS membrane is coated with a thin layer of agarose to keep the planarian moist for up to several hours. In contrast to agarose embedding (see Methods), the agarose used on the PIC plays no role in worm stabilization, and small volumes (~100–200 μ l) are sufficient to provide moisture to the specimen. The planarian is pressed between the PDMS membrane and a gas-permeable plastic film (Biofolie). The PIC is then placed on a glass coverslip for imaging on an upright or inverted microscope (Fig. 1 (A)). Use of an inverted microscope greatly enhances stability because the weight of the chip is on top of the specimen, and all images reported in this paper were taken using an inverted microscope. The PIC enables the manipulation of planarians of various sizes (a few millimeters up to 1–2 centimeters), an important advantage because planarians can vary substantially in size depending on the species as well as environmental factors such as feeding frequency and temperature³⁶. The agarose-coated PDMS membrane and plastic film are not permanently bonded at any point, and peeling apart the two layers releases the worm uninjured within seconds (see Methods). Detailed written and video (Movie S1) protocols for PIC fabrication are provided in the Supplemental Material.

We compared the performance of the PIC to standard methods used in planarian research for immobilization, such as anesthetizing worms with chloretone or ethanol or immobilization in agarose^{16,17}. In all cases, we performed brightfield and fluorescence imaging because *in vivo* studies of planarian regeneration require observation both of anatomical changes in the whole organism and of cellular-level changes in specific structures. Therefore, an effective immobilization technique should provide sufficient stability for brightfield imaging over several hours and for fluorescence imaging for several minutes. Unless otherwise noted, the asexual strain of *Schmidtea mediterranea* was used for all experiments.

Comparison to anesthesia. Three typical protocols for application of anesthetics were compared to mounting on the PIC: long (2.5 hours) exposure to dilute (0.08% by volume) chloretone¹⁶, short (5 minutes) exposure to concentrated (0.2%) chloretone, and 1 hour exposure to 3% ethanol¹⁷. Planarians were kept in the low-concentration chloretone during imaging, but were removed from the high concentration chloretone and the ethanol prior to imaging to minimize toxicity, in keeping with previously published procedures^{16,17}. Under brightfield illumination, all conventional chemical methods led to insufficient

immobilization for proper imaging (Fig. 1 (B, C)), but planarian movement was significantly reduced on the PIC (Fig. 1 (B)). Panels (i–iii) show the standard deviation of ten brightfield images taken ten seconds apart; broader contours on the planarian indicate greater movement. In contrast to (i, ii), the planarian body in (iii) is sharp except for some disturbances around the upper right corner and right eye. These results suggest that the PIC enhances planarian stability during brightfield imaging.

Next, we turned our attention to fluorescence microscopy. Panels (iv–vi) of Figure 1 (B) show the motion of Hoechst 33342-stained worms imaged at UV excitation. Two snapshots were taken 30 seconds apart, colored, and superimposed to show planarian motion between frames; the worm from the initial frame is colored yellow, and the worm from the later frame is colored gray. As expected, worms were more stable under brightfield than under fluorescence illumination in all conditions. Within each condition, worms on the PIC moved significantly less than anesthetized worms.

To further characterize the greater stability of on-chip immobilization, we exposed anesthetized planarians to light at 560 nm (green) and 350 nm (UV), which correspond to the excitation wavelengths of Dextran-Tetramethylrhodamine and Hoechst 33342, respectively, and quantified how long they remained in the field of view. As shown in Fig. 1 (C), worms escaped from the field of view within tens of seconds regardless of the anesthesia protocol. Of the three methods tested, 0.2% chloretone gave the best stability, with mean escape times of 51 seconds at 560 nm excitation and 43 seconds at 350 nm. In addition to providing low stability, chemical anesthetics (especially 0.2% chloretone) often induced planarians to elongate and twist into unusual shapes, making it difficult to orient worms correctly for imaging (Supplemental Fig. S1). Furthermore, anesthetics can cause physical damage (e.g., 3% ethanol damages cilia¹⁷), which might create artifacts in experiments. In summary, Fig. 1 (B), (C) demonstrate that on-chip immobilization is clearly superior to anesthesia because it does not alter the specimen and provides superior sample stability.

Comparison to agarose mounting. Planarians can be physically immobilized by placing specimens in low melting point agarose. Embedding in agarose is a standard technique used for mounting various developmental model organisms and does not have any apparent negative effects on specimen health. The worm becomes trapped after the agarose hardens, enabling relatively stable *in vivo* imaging (Fig. 1 (B), (D), (F)). Physical immobilization, however, is extremely low-throughput, as it takes on the order of 30 minutes for the agarose to solidify. Additionally, planarians can move freely through agarose that is still liquid and often end up in orientations unsuitable for imaging. Removal of planarians without injury also requires dissolving the surrounding agarose in liquid media, which is a slow process.

To compare the stability performance of the PIC with agarose mounting, we took a series of ten minute movies of planarians immobilized on-chip or embedded in agarose when exposed to brightfield and UV light (Movies S2–S5 in the Supplemental Material are samples). For the brightfield movies, planarian movement was quantified by tracking the position of the ocelli over time (Fig. 1 (D), (E)). Tracking was done for five worms immobilized on the PIC, and excellent immobilization stability was observed in all cases. Although we took a total of nine brightfield movies of worms embedded in agarose, we were able to track the eyespots in only four of these nine movies because of issues with orientation or excessive movement (Fig. 1 (D)). In the five unsuitable movies, the planarian either moved its head out of the field of view before the image sequence was completed or was not positioned with the ocelli in view due to movement during mounting. The stability of specimens in the brightfield movies that could be analyzed was comparable to that obtained using the chip (Fig. 1 (D), (E)); in both cases the worm stabilized within



several minutes, as indicated by the plateaus in the plot. These results indicate that agarose achieves similar stability to the PIC for brightfield imaging once worms are immobilized. Agarose mounting, however, is limited by the lower success rate and lower reproducibility. In addition, mounting in agarose is extremely slow (tens of minutes to hours) compared to on-chip immobilization (seconds to minutes), which precludes the use of agarose mounting in high-throughput studies.

As previously done for anesthesia, we characterized worm movement for both immobilization procedures during fluorescence imaging. Specimens in agarose and on the PIC remained in the field of view for minutes, allowing us to evaluate stability by superimposing images from different frames taken 30 seconds, 5 minutes, and 10 minutes apart. These data (Fig. 1 (B)) and a quantification of the center-of-mass motion of the specimen between the time points (Fig. 1 (F) and Supplemental Fig. S2) indicate that movement is significantly less on the PIC. Overall, the PIC provides better stability than agarose-based immobilization for fluorescence microscopy and comparable stability for brightfield microscopy, without the technical limitations of agarose mounting.

In summary, these results demonstrate that although immobilization in agarose is superior to anesthetics for live imaging of planarians, the PIC clearly outperforms both in terms of image quality, reproducibility and ease of use.

Short-term imaging. We then tested whether the stable immobilization achieved by the PIC was sufficient to enable short-term fluorescence imaging at high magnifications. In particular, we investigated the usefulness of the PIC for co-localization studies by taking brightfield and fluorescence images of live planarians at different magnifications and in multiple channels (Fig. 2). The negative phototaxis of planarians is dependent on wavelength, and measurements of the absorption spectra of isolated planarian ocelli indicate an absorbance peak at around 500 nm¹⁵. The sensitivity of the ocelli decreases dramatically beyond 800 nm, and one would ideally use two-photon microscopy in the near-IR to image live planarians. Two-photon microscopes are not widely available, however, and it would be advantageous if imaging could be performed on a standard epifluorescence microscope. We therefore tested the effectiveness of the PIC for immobilizing worms exposed to the standard excitation wavelengths of three commercial dyes (UV (350 nm), blue (480 nm), and green (560 nm) excitation).

As shown in Fig. 2, the PIC enabled high quality *in vivo* imaging in multiple channels and at different magnifications (ranging from 4× to 40×). We imaged stained cell nuclei (Fig. 2 (A, B)) and mitochondria (Fig. 2 (C)) and the planarian gut (Fig. 2 (D)) several hours after the worm had been fed organic beef liver laced with several microliters of fluorescent dye (see Methods and Ref.³⁸). Notably, we obtained quality images at high magnification of the ocelli region (Fig. 2 (B)), which contains the photoreceptors and is therefore the most light sensitive region in the animal at the wavelengths used¹⁵. In addition, we were able to acquire z-stacks of fluorescently labeled anatomical structures in two channels if the label had a strong signal and thus required only short exposures (Fig. 2 (D) and Supplemental Movie S6). These results demonstrate the effectiveness of the PIC for immobilizing planarians for short-term fluorescence *in vivo* imaging.

Post-immobilization recovery. Next, we investigated whether mounting on the PIC had any negative effects on worm health because minimal impact is essential for obtaining longitudinal data on the same sample over long periods of time. To evaluate potential tissue damage from use of the PIC, planarians were immobilized with periodic exposure to green (560 nm) light, continuous brightfield exposure, or with no direct exposure to light for 5 minutes and 1 hour. We also immobilized worms on the PIC for 5 hours in the dark. Worms were imaged before and after immobilization, and each

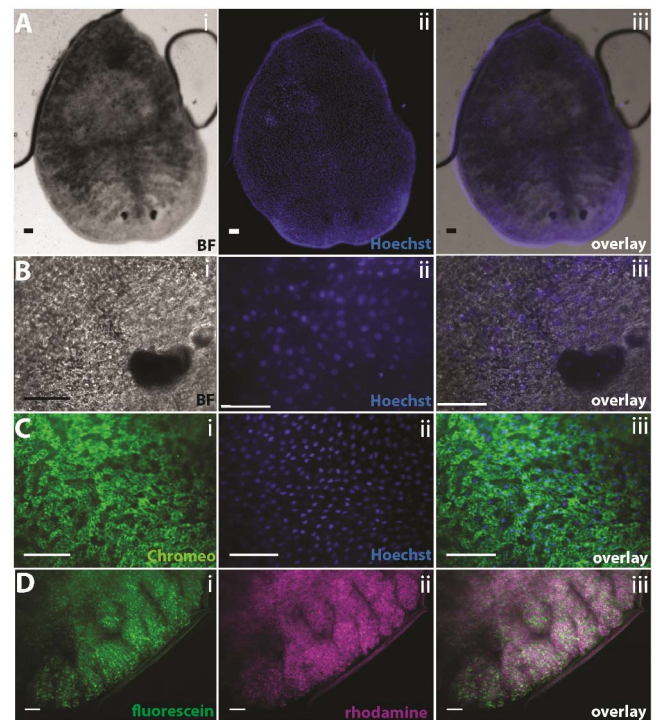


Figure 2 | *In vivo* short-term imaging of planarians. (A) Single capture images of a planarian at 4× magnification. (i) Brightfield (BF) image of the whole worm, (ii) fluorescence image of cell nuclei labeled with Hoechst 33342 and excited at UV, and (iii) overlay of the two images. Exposure times were 4 ms for BF (gain 0, binning 2 × 2) and 50 ms for UV (gain 0, binning 2 × 2). (B) (i–iii) Higher-magnification BF and UV images of a different worm (40×; Hoechst image is a maximum intensity projection of a 12-slice z-stack). Exposure times were 16 ms for BF (gain 0, binning 2 × 2) and 75 ms for UV (gain 0, binning 2 × 2). Individual granules and one of the ocelli are clearly visible in the bottom right corner. (C) Fluorescence images (40×) showing (i) mitochondrial staining (green excitation), (ii) nuclear staining (UV excitation), and (iii) overlay of the two images. Exposure time for each channel was 75 ms (gain 179, binning 2 × 2). (D) Maximum intensity projection of a z-stack of the planarian gut 2–3 hours after it was fed liver containing fluorescein (i) or rhodamine (ii). (iii) Overlay of the two images in which the gut granules and branches are visible in detail. Exposure time for each z-slice was 2 ms for fluorescein and 1 ms for rhodamine (gain 240, binning 2 × 2). Supplemental Movie S6 shows the full z-stack. Scale bars: 50 μm.

image pair was examined for morphological damage resulting from immobilization. No planarians exhibited evidence of significant tissue damage (Fig. 3 (A) shows samples).

In addition to this qualitative assessment of worm health, we quantified the recovery time after immobilization, defined as the time required for planarians to begin moving after release from the PIC (Fig. 3 (B)). Immobilized worms quickly recovered after being imaged. Damage occurred only in cases in which the planarian was improperly mounted or removed (squished or too little water retained). These results confirm that planarians are not injured by the chip and can rapidly recover from on-chip immobilization, even when kept on the PIC for extended periods of time. As such, it appears that worm health is not adversely affected by our procedure, despite the fact that immobilized specimens are not fully immersed in water. The limited impact of the PIC on worm health and the ease of mounting and removing immobilized specimens together suggest that on-chip immobilization could be a valuable method for the acquisition of longitudinal data on the same sample.

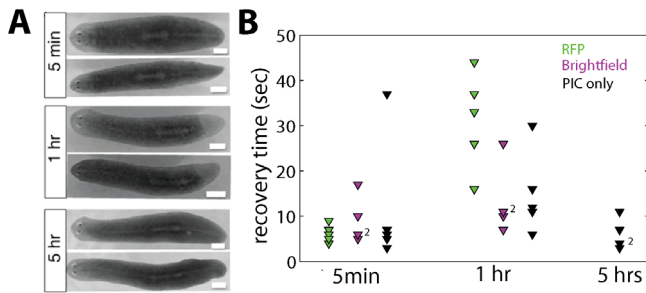


Figure 3 | Post-PIC evaluation of planarian health. (A) Representative images of one worm before and after immobilization. Planarians immobilized on the PIC for 5 minutes, 1 hour, or 5 hours exhibited no visible signs of damage. Scale bars: 500 μ m. (B) Quantitative assessment of the effect of the PIC on planarian health. The recovery time (i.e., the time until the worm started moving after PIC immobilization) is plotted for each time point. Each triangle denotes one experiment; superscripts denote multiple data points. For the first two time points, three conditions were tested: Fluorescence imaging (50 ms exposure, 30 second intervals, 560 nm light), continuous low-light brightfield imaging, and PIC mounting with no direct light.

Head regeneration studies. We applied the PIC to obtain longitudinal data on individual regenerating planarians. We imaged head regeneration at cellular resolution in ten decapitated worms over the course of a week (see Methods). *Dugesia japonica* planarians were used for this experiment because their head is more pronounced compared to *S. mediterranea*. Planarians were amputated on day 0 (Fig. 4 (A)). Beginning one day post-amputation, specimens were mounted on the PIC and imaged in brightfield daily for four consecutive days and again on day 7. We thus obtained five images per worm profiling the dynamics of head regeneration (Fig. 4 (B)). Recovery time following release from the PIC was recorded for all worms. No significant differences in recovery time were observed between consecutive days of imaging (Table 1). Even decapitated planarians are photophobic, and imaging head regeneration is therefore challenging without an adequate immobilization technique. The PIC enabled us to acquire images with sufficient resolution to discern individual cells. With adequate markers it might be possible to use this approach to perform longitudinal regeneration studies of specific anatomical structures.

Wound healing dynamics. Taking advantage of the enhanced sample stability on the PIC, we next studied whether it could be used to study wound closure dynamics in real time. Regeneration begins with wound closure, and characterizing wound healing dynamics in recently injured planarians is an important step toward a comprehensive understanding of regeneration. However, visualization of closure of fresh wounds *in vivo* has not been possible because conventional immobilization techniques require significant

time delay (e.g., the time for the anesthesia to take effect or for agarose to solidify), possess unclear side effects on wound closure dynamics (chemical treatment), and have inherently poor stability (Fig. 1). The PIC is ideally suited for real-time observation of wound healing dynamics because major morphological changes in wound closure happen on the time scale of several hours. Mounting wounded planarians on the PIC is more challenging than mounting intact specimens. We needed 3–5 attempts on average (compared to 1–2 attempts for other imaging applications) to obtain an immobilized worm with sufficient contrast between the surrounding tissue and the wound to enable subsequent image analysis. Despite the multiple attempts required, preparation of a suitable specimen required only 10–15 minutes due to the ease of working with the PIC. We chose brightfield imaging for this initial characterization of wound closure dynamics because it posed less stress on the animal than fluorescence. A fresh wound immediately fills with white mucus after puncture and contrasts with the pigmented (brown) surrounding tissue, allowing for quantitative image analysis of wound closure dynamics (Fig. 5).

We made small wounds in planarians with either a 0.35 mm biopsy punch or a sewing needle immediately before immobilization on the PIC (see Methods for details) and imaged injured specimens in low-intensity brightfield for 2–3 hours. Although we attempted to cause circular wounds, the wounds introduced were elliptical in shape because the planarians began tearing immediately upon wounding. In each case the longer axis of the ellipse was perpendicular to the anterior-posterior axis of the worm. All wounds retained this asymmetry and closed along the longer axis (Fig. 5 and Supplemental Fig. S3). We were unable to introduce wounds that would tear or close preferentially in the anterior-posterior direction, indicating that the anatomy of the worm set the preferred axis. We quantified the change over time in wound area and in the aspect ratio (minor to major axis of an ellipse fitted to the perimeter of each wound) (Fig. 5 (C, D)). Movie S7 in the Supplemental Material shows an example of wound closure. Over the course of 2–3 hours, wounds shrank substantially in area and changed shape from roughly circular to elongated lines, suggesting that wound closure may be anisotropic (wounds close preferentially in the anterior-posterior direction) and that the tensions in the worm are unequal in different directions.

We also performed fluorescence imaging of wound closure dynamics in planarians with Hoechst-labeled nuclei (Movie S8 and Supplemental Fig. S4), demonstrating the feasibility of continuous fluorescence imaging using the PIC. Although long-term imaging in the UV generally has undesirable biological consequences, it may be possible to further characterize wound closure dynamics at sub-cellular resolution using other live stains with other excitation wavelengths. Such data would complement previous histological and immunohistochemical studies, which reported that the initial steps in planarian wound closure involve muscle contractions and epithelial cell migration to cover the wound site^{39–41}. To the best of our knowledge, however, our results are the first *in vivo* observation of the dynamics of planarian wound healing. Further studies on this

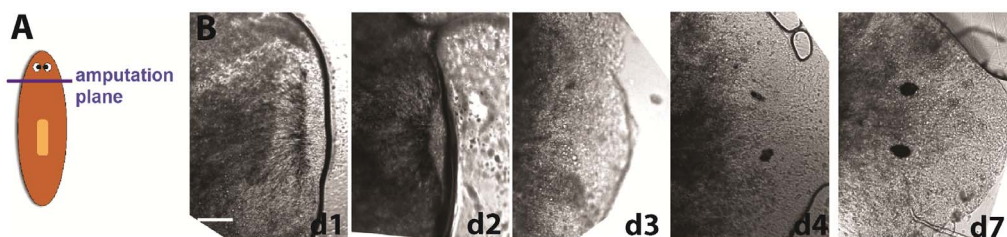


Figure 4 | Planarian head regeneration time course. Ten decapitated *D. japonica* were mounted on the PIC daily for four days and then again on day 7 after amputation. (A) Schematic of the amputation plane. (B) Image sequence showing regeneration of one specimen; images have been rotated so that the head is oriented to the right. Scale bar: 100 μ m.



Table 1 | Worm recovery times after removal from the PIC during the head regeneration assay. No clear trend in recovery times is evident, suggesting that the PIC does not harm the specimen. 3/10 worms died during mounting (due to squishing or drying out). Horizontal mean and s.d. are the average recovery time and variability for individual worms, vertical for all worms on a particular day

Worm #	Day 1	Day 2	Day 3	Day 4	Day 7	mean	s.d.
1	18 s	12 s	10 s	Died mounting	-	13.3 s	4.2 s
2	7 s	8 s	Died mounting	-	-	7.5 s	0.7 s
3	8 s	6 s	7 s	17 s	Died mounting	9.5 s	5.1 s
4	7 s	8 s	7 s	10 s	10 s	8.4 s	1.5 s
5	7 s	7 s	6 s	9 s	10 s	7.8 s	1.6 s
6	13 s	10 s	7 s	10 s	15 s	11 s	3.1 s
7	4 s	6 s	5 s	7 s	6 s	5.6 s	1.1 s
8	12 s	27 s	11 s	12 s	24 s	17.2 s	7.7 s
9	5 s	4 s	13 s	9 s	6 s	7.4 s	3.6 s
10	11 s	12 s	7 s	7 s	12 s	9.8 s	2.6 s
mean	9.2 s	10 s	8.1 s	10.1 s	11.9 s		
s.d.	4.3 s	6.5 s	2.6 s	3.2 s	6.2 s		

topic, made possible by use of the PIC, could deepen the understanding of the relationship between regeneration and wound healing.

Fluorescence imaging of *Hydra*. Finally, we tested the PIC for short-term imaging of *H. vulgaris* to investigate its usefulness outside of planarian research. In contrast to planarians, methods exist for generating transgenic hydras. As such, the primary obstacle for *in vivo* studies of stem cell dynamics and regeneration in *Hydra* has been difficulty with specimen immobilization. *Hydra* were successfully immobilized on the PIC without any modifications to the procedure used for planarians. Fig. 6 shows a transgenic *Hydra* imaged using blue and green excitation at 4× and 10× magnification. Specimen stability was sufficient to allow for the acquisition of 2-channel z-stacks (Fig. 6 (B) is a maximum intensity projection of the z-stack). These results suggest that the PIC may facilitate previously infeasible studies of *Hydra* regeneration.

Discussion

Detailed characterization of stem cell migration and differentiation to regenerate missing or damaged body structures in planarians requires the ability to image live worms with cellular resolution under fluorescent lighting conditions. The photophobia of planarians, however, has greatly hampered *in vivo* studies, and existing

immobilization methods have been inadequate to overcome the challenges posed by these animals. Furthermore, conventional techniques such as immobilization in agarose or anesthesia are either low-throughput (agarose) or have serious side effects (chemicals).

In this paper we present a low-cost (~2 USD per reusable chip), relatively fast on-chip immobilization technique for imaging live planarians. We show that the PIC is superior to all standard immobilization methods for high-magnification brightfield or fluorescence imaging of worms at (sub-)cellular resolution. In addition, on-chip immobilization does not cause serious side effects like anesthetics and is higher throughput than agarose mounting.

Although the development of tissue specific markers using GFP or other protein-specific tags is still ongoing for planarians, this chip allows for initial studies of the dynamics of wound closure and head regeneration. Further optimization of the PIC should enable time-lapse fluorescence imaging of wound closure and regeneration dynamics with sub-cellular resolution. Given the ease of mounting and removing worms, the PIC could potentially be useful in the screening of planarian phenotypes in drug or RNAi studies. Additionally, our device might enable the adaptation of *in vivo* micromanipulation techniques such as laser ablation⁴² to study the real-time dynamics of nervous system regeneration in planarians. We also found that the PIC can be used with no modifications for

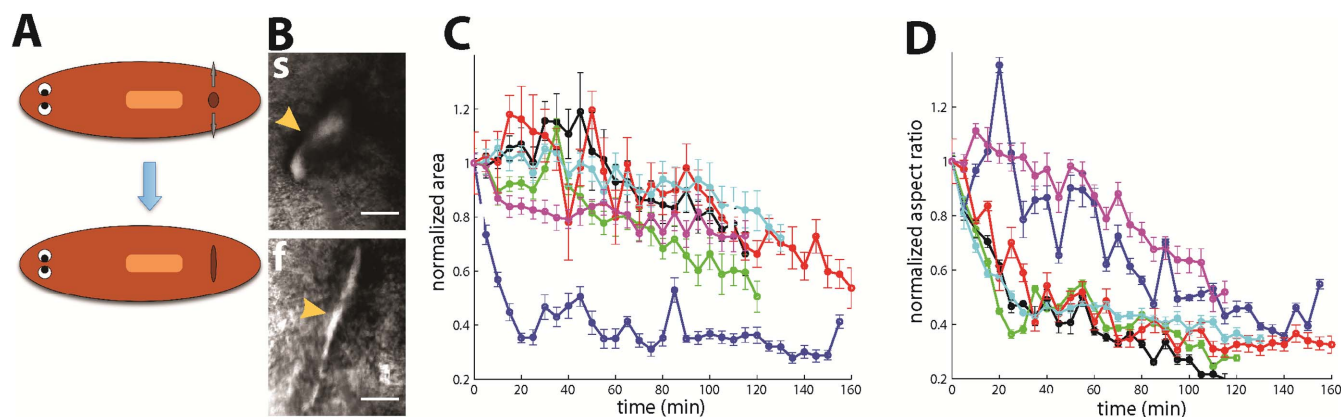


Figure 5 | Wound closure dynamics. (A) Schematic of the wound closure process. (B) Start (s) and final (f) images of a representative data set. Most wounds were not perfect ellipses at the beginning, but all closed along their major axis. Wounds can be identified due to differences in pixel intensity compared to the surrounding tissue. Arrows indicate the locations of the wounds. Scale bars: 100 μ m. (C–D) Analysis of six independent experiments. (C) Plot of the normalized wound area over time, illustrating the decrease in wound size over 2–3 hours on the PIC. Small movements of the immobilized planarian sometimes caused temporary increases in wound area. (D) Ratio of minor to major axis (for an ellipse fitted to the wound in Image) over time. Similar to (C), worm movements caused local peaks in the otherwise decreasing aspect ratio. For clarity, only every fifth value is shown on the area and aspect ratio plots, and the points are connected with a solid line. Error bars denote the standard error of the average of 6–7 analyses of the same wound per planarian.

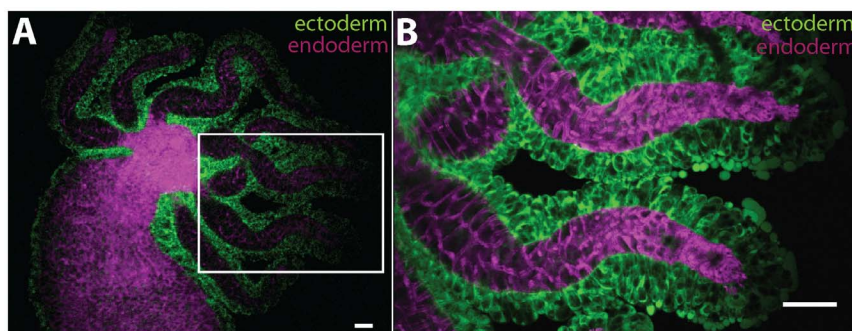


Figure 6 | Fluorescence imaging of live *Hydra*. Transgenic *H. vulgaris* with GFP_ectoderm cells (shown in green) and dsRed2-endoderm cells (shown in magenta). (A) Single slice at 4× magnification. (B) Maximum intensity projection of a 5-slice z-stack at 10× magnification. The tentacles shown in (B) correspond to the boxed region in (A). The exposure times were 19 ms for GFP and 15 ms for RFP (gain: 218) at 4×, and 80 ms for GFP and 50 ms for RFP (gain: 218) at 10×. Scale bars: 100 μm.

the immobilization of *H. vulgaris*, and similar chips may be applied to a range of photophobic organisms.

A major advantage of our method is the lack of chemical or physical alteration of the animal, enabling *in vivo* study of the same specimen multiple times over hours or days to generate dynamic data even without taking time-lapse movies. Application of the PIC may open the field of planarian and *Hydra* regeneration research to developmental biologists who are interested in regeneration dynamics but have avoided these model systems because of the lack of *in vivo* imaging tools.

Methods

Planarian maintenance and fluorescence staining. We used the asexual strain of *Schmidtea mediterranea* for all experiments except for the head regeneration assay, for which we used *Dugesia japonica*. Worms were kept in 1× planarian water¹⁶ in the dark at 20°C except during feeding, cleaning, and experiments. For fluorescent *in vivo* labeling, we used Hoechst 33342, the Chromo live cell mitochondrial staining kit (Active Motif, Carlsbad, CA), dextran-fluorescein (MW 2,000,000; Life Technologies, Grand Island, NY), and dextran-tetramethylrhodamine (MW 2,000,000; Life Technologies). Planarians were incubated for 45 minutes to 1 hour in the stain, washed, and mounted for imaging. 1 mM dextran-fluorescein and dextran-tetramethylrhodamine were mixed with organic liver, and the mixture was fed to planarians that had been starved for one week. Worms were imaged 2–3 hours after feeding. We imaged all specimens on an inverted spinning disc confocal microscope (Olympus DSU, Center Valley, PA) equipped with Slidebook software (version 5, Intelligent Imaging Innovations, Inc., Denver, CO).

Chip fabrication, assembly, and use. The PIC has a PDMS layer, plastic layer, and glass layer (Fig. 1A). The PDMS layer has two components, a “handle” made of solid PDMS with an opening in the center and a thin PDMS membrane stretched across the opening in the handle. The handle was fabricated by casting 20 : 1 base:catalyst PDMS (Sylgard 184, Dow Corning Corporation, Midland, MI) over a metal block several millimeters across. The PDMS handle was cured for at least 1 hour at 75°C. The PDMS membrane was produced by pouring a small amount (less than 1 mL) of 20 : 1 PDMS onto a plate and spreading it uniformly with compressed air. The membrane was cured for 5 minutes at 75°C to partially solidify the PDMS. The handle (opening was then pressed onto the membrane, and the combined device was cured for several hours or overnight at 75°C. After heating, the solid membrane (with the handle attached) was peeled off the plate.

The device was prepared for use by coating the center of the PDMS membrane with 100–200 μL of liquid 2% agarose (Life Technologies) in planarian water. The planarian to be immobilized was then transferred from planarian water to the membrane, and any liquid on the surface of the chip was removed by tapping carefully around the planarian with a Kimwipe. Near-complete drying of the surface is essential for proper immobilization of the worm. The gas-permeable plastic film (Biofolie, Sartorius, Goettingen, Germany) was then gently pressed over the planarian to immobilize it. For imaging the PIC was placed on a glass coverslip with the plastic touching the glass. A single chip can be used multiple times, and only the agarose and Biofolie need to be replaced between experiments. Correct fabrication and use are demonstrated in detail in the video protocol included in the Supplemental Material (Movie S1).

Immobilization using conventional techniques. Planarians were anesthetized with 0.2% chlorotone (5 minutes exposure), 0.08% chlorotone (2 hours exposure), or 3% ethanol (1 hour exposure). Worms were removed from 0.2% chlorotone immediately prior to imaging but kept in 0.08% chlorotone and 3% ethanol during imaging. For the escape time experiments (Fig. 1(C)), anesthetized planarians were observed using the Olympus DSU microscope at 4×, and the time for worms to move completely out of

view was measured using a stopwatch. For physical immobilization, planarians were placed in small glass-bottom dishes (MatTek Corporation, Ashland, MA) in 2% low melting point agarose (Life Technologies) that was still liquid but cool enough not to injure the worms. The dishes were cooled on custom Peltier plates while the agarose solidified to minimize specimen movement. Planarians were imaged after the agarose had solidified completely, which typically was 30 minutes or longer after embedding.

Planarian health assays. For the brightfield experiment, planarians were continuously exposed to light. For the fluorescence experiment, worms were exposed to 560 nm light for 50 ms at intervals of 30 seconds. Worms were removed from the device after immobilization by submerging the PIC in planarian water and gently peeling off the plastic. The recovery time was the interval between the separation of the worm from the immobilization device and its first movement, determined by observation of the worm without magnification and measured with a stopwatch. Worms were imaged in brightfield before and after immobilization to enable characterization of injury (Fig. 3). To investigate the long-term effects of immobilization, planarians were exposed to brightfield light at 30 second intervals for several hours. Following immobilization, worms were kept isolated and observed at least one month later for evidence of morphological damage.

Planarian tracking. Fig. 1 (D),(E) were generated by tracking the position of the planarians’ ocelli. Brightfield tracking movies were taken for 10 minutes with 10 second intervals between frames (Supplemental Movies S2 and S3 are samples for on-chip and agarose immobilization, respectively). The images were thresholded using standard image processing tools in ImageJ (<http://rsb.info.nih.gov/ij/>) to enable tracking of the eyes. The movement value plotted at each time point is the Euclidean distance between the position of the eyes at that time point and its position in the first frame: $d(r1,r2) = \sqrt{(x1 - x2)^2 + (y1 - y2)^2}$. For fluorescence tracking movies, worms were stained with Hoechst 33342 prior to imaging and imaged for 10 minutes with 30 second intervals between frames (Supplemental Movies S4 and S5). Fig. 1 (B) (iv–vi) were generated in ImageJ by superimposing the first two frames (30 seconds apart) of two fluorescence tracking movies. In the superimposed images, the worm from the initial frame is colored yellow, and the worm from the later frame is colored gray. A quantitative analysis of the planarian motion (Euclidean distance between the original center of mass and the center of mass at 30 seconds, 5 minutes, and 10 minutes) is reported in Fig. 1 (F).

***Hydra* maintenance and imaging.** Transgenic *H. vulgaris* were maintained according to standard protocols provided by the Steele lab at UC Irvine⁴³. *Hydra* were raised in *Hydra* medium⁴³ at 18°C in the dark, fed 1×/week with artemia, and cleaned 3×/week. For imaging on the PIC, a specimen that was starved for at least 3 days was mounted on the chip following the same procedure as for planarians. Specimens were imaged on the Olympus DSU microscope.

Head regeneration assay. Ten small *D. japonica* planarians were pre-pharyngeally amputated on day 0 with a razor blade on a cold plate while observed on a standard dissecting microscope. Post-amputation tails were separated into individual petri dishes and stored in the incubator. Beginning on day 1, worms were mounted on the PIC and imaged daily in brightfield at 4× and 10× magnification for four consecutive days. Worms were imaged again on day 7 to confirm that regeneration was complete. Recovery time was measured immediately after each imaging session to assess worm health (Table 1).

Wound closure experiments and data analysis. For wounding a planarian was placed in a 100 mm petri dish. The worm was allowed to orient itself correctly (dorsal side up), and excess water was removed with a plastic transfer pipette to prevent further movement. The planarian was injured post-pharyngeally immediately prior to imaging by puncture with either a 0.35 mm diameter biopsy punch or a sewing needle (diameter 0.88 mm or 1.18 mm, as measured at the thickest part of the needle). The worm was punctured in one fast motion, with the needle or biopsy punch



kept perpendicular to the worm. The size and shape of the resulting wound depended on the size of the puncture device used and the thickness and movement of the specimen. Immediately after wounding, the planarian was mounted onto the PIC following the standard procedure. On average 3–5 attempts were required to obtain a sample with satisfactory immobilization stability and with a wound whose perimeter was clear enough for quantitative image analysis.

The specimen was placed upside down on a confocal slide holder and imaged with either a 4× or 10× objective every 30–45 seconds for 2–3 hours. After imaging, the planarian was removed from the PIC and checked for physical damage on a standard dissecting microscope. Only image sequences of planarians that showed no damage were used for image analysis. Each planarian used in a wound healing experiment was stored in a separate petri dish for at least one week to monitor its health.

The collected image sequences were analyzed in ImageJ to quantitatively characterize changes in the shape and area of the wounds. The intensity of each image in the sequence was thresholded to identify the wound region, which is filled with mucus and therefore lighter than the surrounding tissue. The area and major and minor axis of an ellipse fitted to the perimeter of the wound region were then determined using the Analyze Particles tool. This procedure was repeated at least twice for each image sequence by a single researcher. Multiple individuals also repeated the entire analysis to account for uncertainties in determining the wound region.

1. Reddien, P. W., Oviedo, N. J., Jennings, J. R., Jenkin, J. C. & Sanchez Alvarado, A. SMEDWI-2 is a PIWI-like protein that regulates planarian stem cells. *Science* **310**, 1327–1330, doi:10.1126/science.1116110 (2005).
2. Reddien, P. W. & Sanchez Alvarado, A. Fundamentals of planarian regeneration. *Annu Rev Cell Dev Biol* **20**, 725–757, doi:10.1146/annurev.cellbio.20.010403.095114 (2004).
3. Wagner, D. E., Wang, I. E. & Reddien, P. W. Clonogenic neoblasts are pluripotent adult stem cells that underlie planarian regeneration. *Science* **332**, 811–816, doi:10.1126/science.1203983 (2011).
4. Newmark, P. A. & Sanchez Alvarado, A. Not your father's planarian: a classic model enters the era of functional genomics. *Nat Rev Genet* **3**, 210–219, doi:10.1038/nrg759 (2002).
5. Sanchez Alvarado, A. & Newmark, P. A. Double-stranded RNA specifically disrupts gene expression during planarian regeneration. *Proc Natl Acad Sci U S A* **96**, 5049–5054, doi:10.1073/pnas.96.9.5049 (1999).
6. Newmark, P. A., Reddien, P. W., Cebria, F. & Sanchez Alvarado, A. Ingestion of bacterially expressed double-stranded RNA inhibits gene expression in planarians. *Proc Natl Acad Sci U S A* **100**, 11861–11865, doi:10.1073/pnas.1834205100 (2003).
7. Reddien, P. W., Bermange, A. L., Murfitt, K. J., Jennings, J. R. & Sanchez Alvarado, A. Identification of genes needed for regeneration, stem cell function, and tissue homeostasis by systematic gene perturbation in planaria. *Dev Cell* **8**, 635–649, doi:10.1016/j.devcel.2005.02.014 (2005).
8. Lapan, S. W. & Reddien, P. W. Transcriptome analysis of the planarian eye identifies ovo as a specific regulator of eye regeneration. *Cell Rep* **2**, 294–307, doi:10.1016/j.celrep.2012.06.018 (2012).
9. Liu, S. Y. *et al.* Reactivating head regrowth in a regeneration-deficient planarian species. *Nature* **500**, 81–84, doi:10.1038/nature12414 (2013).
10. Solana, J. *et al.* Defining the molecular profile of planarian pluripotent stem cells using a combinatorial RNAseq, RNA interference and irradiation approach. *Genome Biol* **13**, R19, doi:10.1186/gb-2012-13-3-r19 (2012).
11. Nishimura, O., Hirao, Y., Tarui, H. & Agata, K. Comparative transcriptome analysis between planarian *Dugesia japonica* and other platyhelminth species. *BMC Genomics* **13**, doi:10.1186/1471-2164-13-289 (2012).
12. Robb, S. M., Ross, E. & Sanchez Alvarado, A. SmedGD: the *Schmidtea mediterranea* genome database. *Nucleic Acids Res* **36**, D599–606, doi:10.1093/nar/gkm684 (2008).
13. Sikes, J. M. & Newmark, P. A. Restoration of anterior regeneration in a planarian with limited regenerative ability. *Nature* **500**, 77–80, doi:10.1038/nature12403 (2013).
14. Umesono, Y. *et al.* The molecular logic for planarian regeneration along the anterior-posterior axis. *Nature* **500**, 73–76, doi:10.1038/nature12359 (2013).
15. Azuma, K., Iwasaki, N. & Ohtsu, K. Absorption Spectra of Planarian Visual Pigments and Two States of the Metarhodopsin Intermediates. *Photochem Photobiol* **69**, 99–104, doi:10.1111/j.1751-1097.1999.tb05312.x (1999).
16. Talbot, J. & Schotz, E. M. Quantitative characterization of planarian wild-type behavior as a platform for screening locomotion phenotypes. *J Exp Biol* **214**, 1063–1067, doi:10.1242/jeb.052290 (2011).
17. Stevenson, C. G. & Beane, W. S. A low percent ethanol method for immobilizing planarians. *PLOS ONE* **5**, e15310, doi:10.1371/journal.pone.0015310 (2010).
18. Lucchetta, E. M., Carthew, R. W. & Ismagilov, R. F. The endo-siRNA pathway is essential for robust development of the *Drosophila* embryo. *PLOS ONE* **4**, e7576, doi:10.1371/journal.pone.0007576 (2009).
19. Bernstein, R. W. *et al.* Characterization of fluidic microassembly for immobilization and positioning of *Drosophila* embryos in 2-D arrays. *Sens Actuators A* **114**, 197–203 (2004).
20. Fakhoury, J., Sisson, J. & Zhang, X. Microsystems for controlled genetic perturbation of live embryos: RNA interference, development robustness and drug screening. *Microfluid Nanofluid* **6**, 299–313, doi:10.1007/s10404-009-0405-x (2009).

21. Chung, K. *et al.* A microfluidic array for large-scale ordering and orientation of embryos. *Nat Methods* **8**, 171–176, doi:10.1038/nmeth.1548 (2011).
22. Ghannad-Rezaie, M., Wang, X., Mishra, B., Collins, C. & Chronis, N. Microfluidic chips for *in vivo* imaging of cellular responses to neural injury in *Drosophila* larvae. *PLOS ONE* **7**, e29869, doi:10.1371/journal.pone.0029869 (2012).
23. Ben-Yakar, A., Chronis, N. & Lu, H. Microfluidics for the analysis of behavior, nerve regeneration, and neural cell biology in *C. elegans*. *Curr Opin Neurobiol* **19**, 561–567, doi:10.1016/j.conb.2009.10.010 (2009).
24. Guo, S. X. *et al.* Femtosecond laser nanoaxotomy lab-on-a-chip for *in vivo* nerve regeneration studies. *Nat Methods* **5**, 531–533, doi:10.1038/nmeth.1203 (2008).
25. Zeng, F., Rohde, C. B. & Yanik, M. F. Sub-cellular precision on-chip small-animal immobilization, multi-photon imaging and femtosecond-laser manipulation. *Lab Chip* **8**, 653–656, doi:10.1039/b804808h (2008).
26. Hulme, S. E., Shevkopyas, S. S., Apfeld, J., Fontana, W. & Whitesides, G. M. A microfabricated array of clamps for immobilizing and imaging *C. elegans*. *Lab Chip* **7**, 1515–1523, doi:10.1039/b707861g (2007).
27. Samara, C. *et al.* Large-scale *in vivo* femtosecond laser neurosurgery screen reveals small-molecule enhancer of regeneration. *Proc Natl Acad Sci U S A* **107**, 18342–18347, doi:10.1073/pnas.1005372107 (2010).
28. Rohde, C. B., Zeng, F., Gonzalez-Rubio, R., Angel, M. & Yanik, M. F. Microfluidic system for on-chip high-throughput whole-animal sorting and screening at subcellular resolution. *Proc Natl Acad Sci U S A* **104**, 13891–13895, doi:10.1073/pnas.0706513104 (2007).
29. Chronis, N. Worm chips: microtools for *C. elegans* biology. *Lab Chip* **10**, 432–437, doi:10.1039/b919983g (2010).
30. Crane, M. M., Chung, K. & Lu, H. Computer-enhanced high-throughput genetic screens of *C. elegans* in a microfluidic system. *Lab Chip* **9**, 38–40, doi:10.1039/b813730g (2009).
31. Carvalho, A. *et al.* Acute drug treatment in the early *C. elegans* embryo. *PLOS ONE* **6**, e24656, doi:10.1371/journal.pone.0024656 (2011).
32. Son, S. U. & Garrell, R. L. Transport of live yeast and zebrafish embryo on a droplet digital microfluidic platform. *Lab Chip* **9**, 2398–2401, doi:10.1039/b906257b (2009).
33. Funfak, A., Brosing, A., Brand, M. & Kohler, J. M. Micro fluid segment technique for screening and development studies on *Danio rerio* embryos. *Lab Chip* **7**, 1132–1138, doi:10.1039/b701116d (2007).
34. Wielhouwer, E. M. *et al.* Zebrafish embryo development in a microfluidic flow-through system. *Lab Chip* **11**, 1815–1824, doi:10.1039/c0lc00443j (2011).
35. Pardo-Martin, C. *et al.* High-throughput *in vivo* vertebrate screening. *Nat Methods* **7**, 634–636, doi:10.1038/nmeth.1481 (2010).
36. Dunkel, J., Talbot, J. & Schotz, E. M. Memory and obesity affect the population dynamics of asexual freshwater planarians. *Phys Biol* **8**, 026003, doi:10.1088/1478-3975/8/2/026003 (2011).
37. Chokshi, T. V., Ben-Yakar, A. & Chronis, N. CO₂ and compressive immobilization of *C. elegans* on-chip. *Lab Chip* **9**, 151–157, doi:10.1039/b807345g (2009).
38. Forsthoefel David, J. *et al.* An RNAi Screen Reveals Intestinal Regulators of Branching Morphogenesis, Differentiation, and Stem Cell Proliferation in Planarians. *Dev Cell* **23**, 691–704, doi:10.1016/j.devcel.2012.09.008.
39. Morita, M. & Best, J. B. Electron microscopic studies of planarian regeneration. II. Changes in epidermis during regeneration. *J Exp Zool* **187**, 345–373, doi:10.1002/jez.1401870305 (1974).
40. Schürmann, W. & Peter, R. Inhibition of regeneration in the planarian *Dugesia polychroa* (Schmidt) by treatment with magnesium chloride: a morphological study of wound closure. *Hydrobiologia* **383**, 111–116, doi:10.1023/A:1003475324285 (1998).
41. Pascolini, R., Lorvik, S., Maci, R. & Camatini, M. Immunoelectron microscopic localization of actin in migrating cells during planarian wound healing. *Tissue Cell* **20**, 157–163, doi:10.1016/0040-8166(88)90038-9 (1988).
42. Yanik, M. F. *et al.* Neurosurgery: functional regeneration after laser axotomy. *Nature* **432**, 822, doi:10.1038/432822a (2004).
43. Lenhoff, H. M. *Hydra: Research methods*. (Plenum Press, 1983).

Acknowledgments

The authors thank J.A. Talbot, T.R. Calhoun, D. Yelon, and J. Shaevitz for discussions, S. Quinodoz for help with the video protocol, L. Kang for help with the wound closure data analysis, R. Steele for providing transgenic *Hydra*, and M.A. Thomas and O. Cochet-Escartin for comments on the manuscript. This research was funded by the Lewis-Sigler Fellowship, Burroughs Wellcome Fund CASI Award, and the Alfred P. Sloan Fellowship (to E.-M.S.C.).

Author contributions

J.P.D. and E.-M.S.C. conceived and designed the research. J.P.D., M.B.T., C.H.L. and E.-M.S.C. performed the experiments and analyzed the data. J.P.D. and E.-M.S.C. wrote the manuscript.

Additional information

Supplementary information accompanies this paper at <http://www.nature.com/scientificreports>



Competing financial interests: The authors declare no competing financial interests.

How to cite this article: Dexter, J.P., Tamme, M.B., Lind, C.H. & Collins, E.-M.S. On-chip immobilization of planarians for *in vivo* imaging. *Sci. Rep.* **4**, 6388; DOI:10.1038/srep06388 (2014).



This work is licensed under a Creative Commons Attribution-NonCommercial-NoDerivs 4.0 International License. The images or other third party material in

this article are included in the article's Creative Commons license, unless indicated otherwise in the credit line; if the material is not included under the Creative Commons license, users will need to obtain permission from the license holder in order to reproduce the material. To view a copy of this license, visit <http://creativecommons.org/licenses/by-nc-nd/4.0/>